Anomalous Magnetic Properties Near the Spin-Flop Bicritical Point in Mn_2AS_4 (A = Si and Ge)

K. Ohgushi and Y. Ueda

Institute for Solid State Physics, University of Tokyo, Kashiwa, Chiba 277-8581, Japan

(Received 11 July 2005; published 14 November 2005)

The magnetic properties of the single crystalline Mn_2AS_4 (A = Si and Ge) with an olivine structure, which are the uniaxially anisotropic antiferromagnets (the b axis as an easy axis), were investigated. Near the Néel temperature, both compounds exhibit the contrastive magnetic responses along the c axis, namely, the spontaneous weak ferromagnetism in A = Si and the significant enhancement of the differential susceptibility (dM/dH) under the small magnetic field in A = Ge. When A = Ge, we also observed the evolution of dM/dH along the a axis at low temperatures. We discuss these phenomena on the basis of the magnetic field-temperature (H-T) phase diagram with the spin-flop bicritical point (H_{BP}, T_{BP}). The role of the thermal or quantum fluctuation was stressed.

DOI: 10.1103/PhysRevLett.95.217202 PACS numbers: 75.40.−s, 75.30.Gw, 75.30.Kz

The anisotropic antiferromagnet under an external magnetic field has been well investigated for several decades as an ideal playground to study the multicritical phenomena [1–5]. When the uniaxially anisotropic antiferromagnet on the bipartite lattice is subject to the external magnetic field along the spin easy axis, the first-order spin-flop (SF) transition occurs at a certain magnetic field, H_{SF}. The first-order line in the magnetic field-temperature (H-T) plane terminates at the bicritical point (BP) (H_{BP}, T_{BP}), from which 2 second-order lines emerge. One of them separates the antiferromagnetic (AF) phase from the paramagnetic (PM) phase and exhibits the Ising-like criticality, whereas the other between the SF and PM phases shows the XY-like critical behavior. Importantly, the criticality at the bicritical point is described by the Heisenberg one [1]. The experiments on $GdAlO_3$ [2] and $MnCl_2 \cdot 4H_2O$ [3] confirmed these pictures. Then, the research has been extended to the antiferromagnet on the *frustrated* lattice. It was demonstrated that $CsNiCl_3$ exhibits the H-T phase diagram with a novel multicritical point [4] and its criticality was analyzed by the scaling theory dealing with the spin chirality [5]. It is expected that further exotic multicritical phenomena will appear in the anisotropic antiferromagnet on the nontrivial lattice. In this Letter, we report the unusual suppression of H_{SF} near Néel temperature (T_N) in the olivine-type compounds, Mn_2AS_4 (A = Si and Ge). Combined with the peculiar structure of the magnetic point group with regard to the direction of the magnetic moment, this suppression results in the weak ferromagnetism (WF) in A = Si and the enhancement of the differential susceptibility (dM/dH) in A = Ge.

The olivine structure (Fig. 1) with the chemical formula B_2AX_4 takes the $Pnma$ orthorhombic symmetry. B sites consist of the two crystallographically independent sites (4a and 4c sites) and form the triangle-based one-dimensional chain structure (sawtooth chain) through the edge-sharing bonds along the b axis [Fig. 1(b)]; therefore, a geometric magnetic frustration exists [6]. Each chain structure is connected with each other through the corner-sharing bonds in the ac plane, forming the three-dimensional network. When the magnetic unit cell is identical to the crystallographic one, the possible magnetic structures were classified by the representation analysis and the results are summarized in Table I [7]. Among a number of olivine-type compounds, the system with Mn^{2+} ion as B site is rather suitable to study the magnetic properties inherent in the olivine structure, because Mn^{2+} ion possesses no orbital degeneracy. It was reported that Mn_2SiS_4 shows the WF in the very narrow temperature region (83–86 K) just below T_N [8]. The powder neutron diffraction measurements revealed that the spins take the $C_y - C'_y$ arrangement (antiparallel arrangement of spins at 4a and 4c sites along the b direction; see Fig. 1(b)] at the

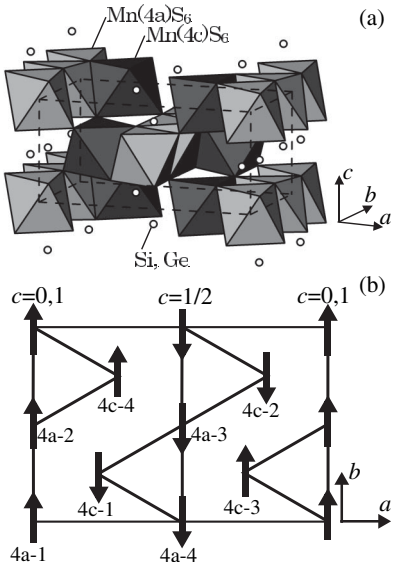

FIG. 1. The olivine structure. (a) Mn^{2+} ions share two crystallographically inequivalent sites (4a and 4c sites) and are coordinated octahedrally by sulfurs. The octahedra share corners as well as edges with each other, forming the three-dimensional network. The broken line represents the primitive unit cell. (b) The $C_y - C'_y$ spin structure projected onto the ab plane. Only the nearest-neighbor links, corresponding to the edge-sharing network, are shown.

TABLE I. The magnetic structures of the irreducible representations (Γ_i) for *Pnma* space group. M denotes the magnetic point group. A_i, F_i, C_i, and G_i ($i = x$, y, and z) are defined as $A_i = S^{4a}_{1,i} - S^{4a}_{2,i} - S^{4a}_{3,i} + S^{4a}_{4,i}$, $C_i = S^{4a}_{1,i} + S^{4a}_{2,i} - S^{4a}_{3,i} - S^{4a}_{4,i}$, $G_i = S^{4a}_{1,i} - S^{4a}_{2,i} + S^{4a}_{3,i} - S^{4a}_{4,i}$, and $F_i = S^{4a}_{1,i} + S^{4a}_{2,i} + S^{4a}_{3,i} + S^{4a}_{4,i}$, where $S^{4a}_{j,i}$ is the ith component of the spin at 4a-j site [Fig. 1(b)]. A'_i, F'_i, C'_i, and G'_i ($i = x$, y, and z) are defined for the spins at 4c site in the similar manner.

			Transition elements					
			4a				4c	
Γ_i	M	Generators						
Γ_{1g}	mmm	$2_x, 2_z, \bar{1}$	G_x	C_y	A_z	$\cdots$	C'_y	$\cdots$
Γ_{2g}	mmm	$2_x, 2_z, \bar{1}$	C_x	G_y	F_z	C'_x	$\cdots$	F'_z
Γ_{3g}	mmm	$2_x, 2_z, \bar{1}$	F_x	A_y	C_z	F'_x	$\cdots$	C'_z
Γ_{4g}	mmm	$2_x, 2_z, \bar{1}$	A_x	F_y	G_z	$\cdots$	F'_y	$\cdots$
Γ_{1u}	mmm	$2_x, 2_z, \bar{1}$	$\cdots$	$\cdots$	$\cdots$	G'_x	$\cdots$	A'_z
Γ_{2u}	mmm	$2_x, 2_z, \bar{1}$	$\cdots$	$\cdots$	$\cdots$	$\cdots$	G'_y	$\cdots$
Γ_{3u}	mmm	$2_x, 2_z, \bar{1}$	$\cdots$	$\cdots$	$\cdots$	$\cdots$	A'_y	$\cdots$
Γ_{4u}	mmm	$2_x, 2_z, \bar{1}$	$\cdots$	$\cdots$	$\cdots$	A'_x	$\cdots$	G'_z

ground state, that the G_x contribution develops with elevated T, and that the spins orient to the a axis with the $C_x - C'_x$ spin structure near T_N [9]. According to these results, the irreducible representation belonged by the spin system changes from Γ_{1g} at the ground state to Γ_{2g} near T_N. Whereas Γ_{1g} irreducible representation prohibits the appearance of WF along any directions, the ferromagnetic components (F_z and F'_z) are allowed to emerge in the Γ_{2g} irreducible representation (Table I). The neutron diffraction measurements have actually observed the weak $F_z - F'_z$ contribution near T_N [9]. Replacement of Si with Ge was reported not to introduce any dramatic change in the T dependence of the magnetic susceptibility or the neutron diffraction profile at the ground state [8,10]. It should be noted that the previous studies are restricted to the polycrystals and lack information on the anisotropy. Moreover, it is still unclear how the magnetic structure belonging to the Γ_{2g} irreducible representation is stabilized only near T_N.

Single crystals of Mn_2AS_4 (A = Si and Ge) with the typical dimensions of 1 mm × 1 mm × 1 mm were grown by the chemical vapor transport method with I_2 as a transport agent [11]. The lattice parameters were evaluated by the x-ray powder diffraction method to be $a = 12.693(5)$ Å, $b = 7.431(3)$ Å, $c = 5.940(2)$ Å for A = Si and $a = 12.796(4)$ Å, $b = 7.451(3)$ Å, $c = 6.034(2)$ Å for A = Ge. The data of magnetization were collected using the SQUID magnetometer. The specific heat measurements were performed in the commercial setup with the use of the relaxation method.

First, we concentrate on A = Si. Figures 2(a)–2(c) represent the T dependence of the magnetization (M) divided by the external magnetic field (H) for various magnetic fields along the a, b, and c axes. Here, the detected M is parallel to the applied H. The curve at 5 T for every direction shows the similar T dependence. It has a tiny kink structure at T_N (= 86 K) and saturates toward the constant value at the lowest T. The effective magnetic moment estimated from Curie-Weiss fit is $p = 5.91$, being closer to the theoretical value for $S = 5/2, 5.92$. Curie-Weiss (CW) temperature is also obtained as $\theta_{CW} = -246$ K, thereby the ratio $|\theta_{CW}|/T_N$ (= f) is 2.86. This is much smaller than 12 in Mn_2SiO_4 [6], indicating that a geometrical frustration is relaxed in the chalcogenide.

M/H along the b axis at 0.1 T steeply decreases with lowering T [Fig. 2(b)]. This feature is more clearly seen in the M-H curve at 5 K [Fig. 2(g)] and indicates a uniaxial anisotropy with the b direction as an easy axis, which is consistent with the neutron diffraction measurements [9]. The evolution of the magnetization around 3 T corresponds to the first-order spin-flop transition from the b axis to the a or c axis. To obtain the phase diagram in H-T plane, we take the isothermal magnetization curves at various temperatures and plot dM/dH in Fig. 3(a). The magnetic fields with the largest dM/dH are set to be the phase boundaries

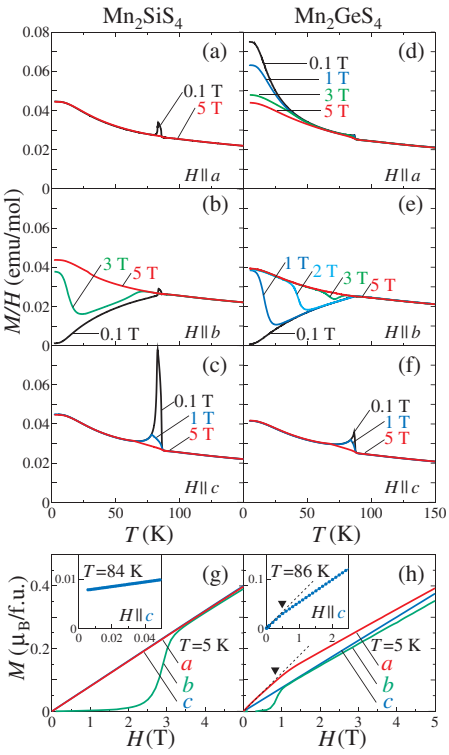

FIG. 2 (color). (a)–(f) Temperature dependence of the magnetization (M) divided by the external magnetic field (H) at various magnetic fields along the a [(a) and (d)], b [(b) and (e)], and c axes [(c) and (f)] for Mn_2SiS_4 [(a)–(c)] and Mn_2GeS_4 [(d)–(f)]. M is detected along the same direction as H. (g), (h) Isothermal magnetization curves at 5 K for Mn_2SiS_4 (g) and Mn_2GeS_4 (h). The data along the c axis near the Néel temperature are shown in the insets, in which abscissa and ordinate scales are different between Mn_2SiS_4 and Mn_2GeS_4. The dotted lines in (h) depict the linear extrapolation from the curves at low magnetic field and the closed triangles represent the points where the deviation of the experimental curve from the dotted line becomes prominent.

between the AF and SF phases. We also measure the T dependence of M/H at various magnetic fields near T_N to acquire the phase boundaries between the PM and AF/SF phases. We depict the obtained phase diagram in Fig. 3(c). Compared with conventional uniaxial antiferromagnets [2], the peculiar feature of Fig. 3(c) is that H_{SF} shows steep decrease near T_N, which is unambiguously responsible for the appearance of the WF near T_N. As clearly seen in Fig. 2(c), the WF is along the c axis in accordance with the previous neutron diffraction measurements [9]. The spontaneous magnetization is estimated to be $0.042\mu_B/Mn^{2+}$ at 84 K [inset of Fig. 2(g)]. To clarify how the WF emerges, or equivalently, the spin structure changes between $C_x - C'_x$ and $C_y - C'_y$ as the function of T, it is necessary to know where the first-order line terminates in the H-T plane more precisely. When we extrapolate the first-order line in the natural manner, we notice that it meets the $H = 0$ line at a certain temperature T' ($\sim$ 83.5 K), where the magnetic structure is expected to change from $C_y - C'_y$ to $C_x - C'_x$ with increasing T. Because each arrangement belongs to the different irreducible representation (Γ_{1g} and Γ_{2g}, respectively), the transition at T' should be first order. This kind of spin-reorientation transition is observed in Fe_2GeS_4 [12,13], where the spins reorient from the b to the a axis with *decreasing* T. To find the signature of such successive phase transition, we carried out the specific heat measurements. As seen in Fig. 4(b), there is only one peak structure corresponding to the antiferromagnetic transition without any other anomaly. This result indicates that the change from the $C_y - C'_y$ to the $C_x - C'_x$ spin structure at $H = 0$ is not the thermodynamic transition but the crossover. The magnetization along the c axis [Fig. 4(a)] is expressed as $M_c(H, T) = M_c^0(T) + \chi_{cc}(T)H$, where M_c^0 is the spontaneous magnetization with the maximum value just below T_N and the nonvanishing values at any T, and χ_{cc} is the T dependent linear susceptibility of the monotonic function about T. The finite M_c^0 outside the T region of $T' < T < T_N$ also supports the view on the spin structure change as the crossover. The reason why the first-order line does not extend to $H = 0$ line is not clear at present; however, it may be relevant to the strong thermal fluctuation near T_N.

We estimate the critical exponent α by fitting the specific heat (C) near T_N with the function

$$C^{\pm} = \frac{A^{\pm}}{\alpha^{\pm}}|t|^{-\alpha^{\pm}} + B + Et, \quad (1)$$

where $t = (T - T_N)/T_N$ and the superscript $+(-)$ refers to $t > 0$ ($t < 0$). The first term on the right-hand side represents the leading contribution to the singularity and the others express the regular ones. The fitted results are shown in the inset of Fig. 4. When $\alpha^{\pm} > 0$, we obtain $\alpha^+ = 0.35(10)$, $\alpha^- = 0.13(5)$; however, a large discrepancy between α^+ and α^- is in contradiction to the renormalization group theory. Meanwhile, on the assumption of $\alpha^{\pm} < 0$, we get $\alpha^+ = -0.06(3)$, $\alpha^- = -0.03(2)$. These values are comparable to the critical exponent of the Heisenberg universality class, $\alpha = -0.116$. This result also supports that the critical phenomena of this compound is related to the bicritical point.

We proceed to A = Ge and represent the magnetic properties for it in Figs. 2(d)–2(f) and 2(h). The overall features

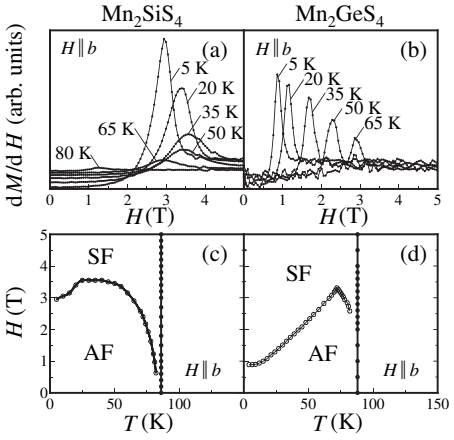

FIG. 3. (a), (b) Differential magnetic susceptibility (dM/dH) for Mn_2SiS_4 (a) and Mn_2GeS_4 (b). (c), (d) The magnetic field-temperature (H-T) phase diagram for Mn_2SiS_4 (c) and Mn_2GeS_4 (d). The magnetic field is applied along the b axis. The open circles are determined by the isothermal magnetization curves and represent the first-order line of the spin-flop transition. The closed circles are obtained by the temperature dependence of M/H and represent the second-order line between the paramagnetic and magnetic phases. SF and AF stand for the spin-flop and antiferromagnetic phases, respectively.

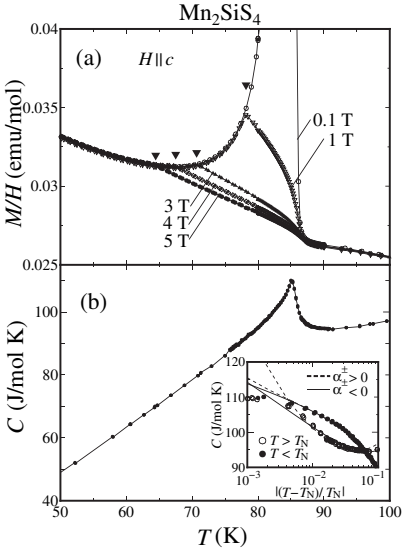

FIG. 4. (a) Temperature dependence of the magnetization (M) divided by the external magnetic field (H) at various magnetic fields along the c axis for Mn_2SiS_4. The closed triangles denote the cusp structures. (b) The specific heat (C) at zero magnetic field for Mn_2SiS_4. The inset shows the data near the Néel temperature (T_N) and the results of the theoretical fits with Eq. (1). The solid (broken) line corresponds to $\alpha^{\pm} < 0$ ($\alpha^{\pm} > 0$).

of M/H are similar to those of $A =$ Si. The ratio f is estimated to be 2.30 ($T_N = 88$ K, $\theta_{CW} = 202$ K). Taking the same procedure as in $A =$ Si, we obtain the H-T phase diagram for the spin-flop transition shown in Fig. 3(d). H_{SF} takes the relatively small value, 0.89 T at 4 K, gradually increases with elevated T, and shows the abrupt decrease near T_N.

The M/H curves along the c axis under low magnetic fields (say 0.1 T) show enhancement just below T_N as in $A =$ Si [Fig. 2(f)] and this is relevant to the suppression of H_{SF} near T_N. However, in contrast to $A =$ Si, no spontaneous magnetization is observed [inset of Fig. 2(h)]. This infers that the first-order line of the spin-flop transition does not meet the $H = 0$ line, but terminates at the bicritical point with finite H_{BP} on the second-order lines, although we could not determine the definite position of it from our experimental data. At the bicritical point, the $C_x - C'_x$, $C_y - C'_y$, and $C_z - C'_z$ spin arrangements are equally developed due to its Heisenberg criticality, and the WF along the c and a axes concomitantly emerges since the $C_x - C'_x$ and $C_z - C'_z$ structures belong to the Γ_{2g} and Γ_{3g} irreducible representations, respectively. It is likely that the enhancement of dM/dH near T_N in the experiments corresponds to the critical fluctuation toward the WF realized at the bicritical point. The absence of the enhancement of dM/dH along the a axis in our experiments should be explained by the further minor factors (e.g., the effect of orthorombicity). The M-H curve along the c axis at 86 K [inset of Fig. 2(f)] indicates that the enhancement of dM/dH is gradually suppressed with increasing H. This is understood as the critical fluctuation is not discerned when the system is far from the bicritical point among the H_a-H_b-T manifold (H_i being the ith component of H).

In $A =$ Ge, M/H along the a axis also enhances at low T and low H [Figs. 2(d) and 2(h)]. This corresponds to the small H_{SF} at this T region [Fig. 3(d)] and means the system is quite near the magnetically ordered state with the $C_z - C'_z$ spin arrangement. It is remarkable that there is a difference between the direction of the enhanced dM/dH near T_N and that at the low T. One possible origin of it is the different nature of the fluctuation, that is, the thermal fluctuation near T_N and both the thermal and quantum fluctuations at the ground state. The M-H curve along the a axis at 5 K [Fig. 2(h)] indicates that the enhancement of dM/dH gradually disappears with increasing H. This should be understood in the same manner as the M-H curve along the c axis at 86 K.

We discuss both $A =$ Si and Ge systems on the same footing. All the differences in the magnetic properties are reduced to that of the phase diagrams depicted in Figs. 3(b) and 3(d); nevertheless we could not address its origin at present, because the key ingredient which determines the magnitude and the T dependence of H_{SF} is unclear in these compounds. We have discussed that the enhancement of M/H is the reflection of the thermal or quantum fluctuation toward the WF state. This scenario seems to be in contrast to the order by disorder in the geometrically frustrated magnets [14], where the thermal or quantum fluctuations prefer the collinear spin arrangements. Our results indicate that both fluctuations can play a various role in the system that has the moderate magnetic anisotropies and a characteristic structure of the magnetic point group with regard to the direction of the magnetic moments on the geometrically frustrated lattice.

To summarize, we have investigated the anisotropic magnetic properties of the single crystalline Mn_2AS_4 ($A =$ Si and Ge). We depicted the magnetic field-temperature (H-T) phase diagram ($H \parallel b$) for the spin-flop transition and clarified that the spin-flop field, H_{SF}, exhibits a steep decrease near Néel temperature (T_N). This results in the spontaneous weak ferromagnetism and the significant enhancement of the differential susceptibility (dM/dH) along the c axis in $A =$ Si and Ge, respectively. When $A =$ Ge, we also observed the evolution of dM/dH along the a axis at low temperature. In these phenomena, the thermal and/or quantum fluctuations have a crucial role.

We are grateful to Z. Hiroi and J. Yamaura for their help in measuring the specific heat and taking the x-ray Laue photograph, respectively. One of the authors (K. O.) is supported by the Japan Society for the Promotion of Science for Young Scientists.

[1] M. E. Fisher and D. R. Nelson, Phys. Rev. Lett. **32**, 1350 (1974); J. M. Kosterlitz, D. R. Nelson, and Michael E. Fisher, Phys. Rev. B **13**, 412 (1976).
[2] H. Rohrer, Phys. Rev. Lett. **34**, 1638 (1975); H. Rohrer and C. Gerber, *ibid.* **38**, 909 (1977).
[3] R. A. Butera, L. M. Corliss, J. M. Hastings, R. Thomas, and D. Mukamel, Phys. Rev. B **24**, 1244 (1981).
[4] P. B. Johnson, J. A. Rayne, and S. A. Friedberg, J. Appl. Phys. **50**, 1853 (1979).
[5] H. Kawamura, A. Caille, and M. L. Plumer, Phys. Rev. B **41**, 4416 (1990); H. Kawamura, J. Phys. Condens. Matter **10**, 4707 (1998).
[6] I. S. Hagemann, P. G. Khalifah, A. P. Ramirez, and R. J. Cava, Phys. Rev. B **62**, R771 (2000).
[7] E. F. Bertaut, Acta Crystallogr. Sect. A **24**, 217 (1968).
[8] G. Lamarche, F. Lamarche, and A.-M. Lamarche, Physica (Amsterdam) **194-196B**, 219 (1994).
[9] A.-M. Lamarche, G. Lamarche, C. Church, J. C. Woolley, I. P. Swainson, and T. M. Holden, J. Magn. Magn. Mater. **137**, 305 (1994).
[10] T. Duc, H. Vincent, E. F. Bertaut, and V. V. Qui, Solid State Commun. **7**, 641 (1969).
[11] J. Fuhrmann and J. Pickardt, Acta Crystallogr. Sect. C **45**, 1808 (1989).
[12] H. Vincent and E. F. Bertaut, J. Phys. Chem. Solids **34**, 151 (1973).
[13] A. Junod, K.-Q. Wang, G. Triscone, and G. Lamarche, J. Magn. Magn. Mater. **146**, 21 (1995).
[14] C. L. Henley, Phys. Rev. Lett. **62**, 2056 (1989).